ISSN 2075-1087, Gyroscopy and Navigation, 2019, Vol. 10, No. 2, pp. 90–98. © Pleiades Publishing, Ltd., 2019.
Russian Text © The Author(s), 2019, published in Giroskopiya i Navigatsiya, 2019, No. 1, pp. 93–106.

# Selected Features of Autonomous Underwater Robot Dynamics under Near-Bottom Equidistant Motion Control

**L. V. Kiselev[a], * and A. V. Medvedev[a]**

[a] *Institute of Marine Technology Problems, Far-East Branch, Russian Academy of Sciences (IMTP FEBRAS), Vladivostok, 690091 Russia*

******e-mail: kiselev@marine.febras.ru*

Received December 11, 2018; revised February 13, 2019; accepted February 13, 2019

**Abstract**—Search and survey missions of an autonomous underwater robot are usually associated with motion along equidistant trajectories near the bottom. The most difficult problem here is to control motion in a vertical plane in presence of obstacles in the bottom relief along the motion route. When the obstacles are detected using a multi-channel front-viewing echolocation system, equidistant motion of the vehicle is provided with tracking of the bottom relief profile. The dynamic model of motion with specific requirements for the structure and control parameters is studied. Comparative analysis of the dynamic properties of control system depending on the design and functional features of the actuating elements and the range-measuring echolocation system is presented.

*Keywords:* underwater robotics, autonomous underwater vehicles (robots), motion control, dynamic models, bottom relief

**DOI:** 10.1134/S2075108719020044

## INTRODUCTION

In the applications where an autonomous underwater vehicle or robot (AUV/AUR) is used for sonar scanning and photography of the bottom relief, hydrophysical surveys in the near-bottom area, and bottom objects examination, it is necessary to provide its motion along the path equidistant to the bottom, bypassing or avoiding the obstacles. To determine the distances to the bottom and to detect the obstacles, high-resolution multi-channel sonar systems or multibeam sonars are used. Equidistant motion is controlled by means of adjustable program which predicts the spatial trajectory and orients the vehicle along it. Readings from the sonar are used in constructing the control algorithm to approximate the visible part of the relief by plane areas. Each surface area is described by geometrical parameters in a coordinate system fixed to the vehicle's body. The entire trajectory is represented as a number of segments, each minimizing the length of the equidistant path relative to adjacent flat elements at a current point of the trajectory. In case of a flat surface, the problem is simplified and reduced to stabilization of positional and angular misalignments formed by means of a few range-finders. A similar method of control has been implemented in different modifications in most of the vehicles designed by the IMTP FEBRAS [1–4].

In most cases, the sonar survey is carried out when the AUV is moving at a distance of 20–40 m from the bottom surface, while photo- or video shooting or profile scanning of the bottom are performed at a distance of 3 to 5 m. Motion in vertical plane is most difficult in terms of dynamics and control methods. Specific dynamics of the control system in different modes of AUV motion are discussed in [5–7]. When the bottom relief is variable, with slope angles up to 20°–25° and the depth gradients of 20–25 m, it is essential to provide an equidistant trajectory of the vehicle in course of sonar survey, profile scanning, or photo and video shooting, for two main modes:

- motion along a slope with zero trim, or with a trim corresponding to the slope angle;
- obstacle avoidance on the move at a constant or variable speed.

To minimize the energy consumed during motion, the mode with the minimum hydrodynamic resistance is obviously preferable in order to ensure some "optimal" attack angle corresponding to specified actual speed. When moving with zero trim along a slope, large attack angles are possible, and the energy consumption can be reduced only by decreasing the speed. Similarly, it is difficult to provide an optimal energy-saving mode during complex maneuvering near an obstacle, because in such situation the vehicle's safety is of top priority; therefore, additional energy is consumed for motion. Another specific feature of this problem is incomplete, fuzzy information on the bottom relief, which makes it reasonable to construct a

hybrid control structure with fuzzy logic elements. These issues were discussed in detail in [2, 5, 6], and the results of these studies are applicable to solving the problems of equidistant motion control when operating an AUV in the conditions of complex bottom relief, with obstacles avoidance "on the move".

Some specific features of control, associated with the speed changing from zero to the maximum value, are also worth mentioning. It is evident that with increasing speed the efficiency of hydrodynamic forces becomes higher, in which case the motion is associated with small attack angles and hence, in some cases, gives a gain in energy consumption. At small speed, the efficiency of hydrodynamic resistance reduces and, moreover, depth controllability worsens down to inverse controllability. According to the design and experimental data, the latter effect occurs within the speed range from 0.15 to 0.20 m/s [2].

The control based on echo sounding data from the forward-looking systems can be used for overcoming relatively low single obstacles. When an obstacle is detected, a torque proportional to the ratio of measured distances is created, and the vehicle moves with a trim corresponding to the obstacle height and to the distance at which the maneuver starts. At the same time, as the vehicle is approaching an obstacle, some safety distance is controlled to ensure the possibility for obstacle avoidance "on the move" without changing the speed. The motion mode is chosen depending on the slope steepness which is calculated based on the data from the sonar station at each point of the trajectory [2, 4].

## DYNAMIC MODEL OF AUV MOVING IN VERTICAL PLANE

In a number of known works (e.g. [7, 8]), the dynamics of an underwater vehicle is described using an extended state vector the components of which are the positional and angular speed relative to the rotation axes bound to the vehicle. Similar scheme is used in some foreign studies generally dedicated to kinematic correlations between the forces affecting the vehicle, and the motion parameters [9–11]. An AUV dynamics is traditionally described using "natural" coordinates directly associated with hydrodynamic processes and with constructing the control algorithms [1–6, 12, 13]. Taking this into account, we represent a mathematical model of AUV motion in vertical plane as a system of equations reflecting the interaction between all hydrostatic, hydrodynamic and control forces:

$$\begin{aligned} m_x\dot{v} &= R_x(v,\alpha) + P\sin\vartheta + T_{x1}\cos\alpha - T_{y1}\sin\alpha,\\ m_y v\dot{\vartheta} &= R_y(v,\alpha,\dot{\psi}) + P\cos\vartheta + T_{y1}\cos\alpha + T_{x1}\sin\alpha,\\ I_{zz}\ddot{\psi} &= M_0\sin\psi + M_z(v,\alpha,\dot{\psi}) + M_{z\,\mathrm{cont}},\\ \dot{X} &= v\cos\vartheta,\quad \dot{Y} = -v\sin\vartheta,\quad \psi = \vartheta + \alpha. \end{aligned} \tag{1}$$

Designations in the equations (1) are taken from the works mentioned above, in particular: $OXY$ is local coordinate system, $Y$ is submersion depth; $Axy$ is velocity (flow rate) coordinate system; $Ax_1y_1$ is the vehicle-fixed coordinate system; $v$ is the speed relative to inflow, $\psi$ is the trim, $\alpha$ is the angle of incidence, $\vartheta$ is the angle of trajectory; $m_x$, $m_y$, $I_{zz}$ are the masses and the vehicle's body inertia moment, taking into account the added-liquid mass; $R_x$, $R_y$, $M_z$ are hydrodynamic forces and torque; $M_0$ is stability torque; $T_{x1}$, $T_{y1}$, $M_{z\,\mathrm{cont}}$ are the projections of control forces and torques in the vehicle-fixed coordinate system; $P$ is variable buoyancy depending, in particular, on the vehicle submersion depth.

The dynamic properties of the system described by equation (1) were studied by means of virtual hydrodynamics by example of a 3D computer model of a medium-class AUV sketched in Fig. 1. The following characteristics and parameters of AUV were taken as the initial data: geometrical parameters (length, diameter and volume of the hull, linear dimensions of rear fins, dimensions of projecting parts), inertial parameters (vehicle weight and inertia moment, taking into account the added-liquid masses and inertia moments of liquid).

The list below specifies some technical specifications of the AUV, which determine its dynamic properties:

- volume $V$ (draught), $m^3$: 0.49;
- weight components $m_x$, $m_y$, kg: 558, 720;
- inertia moment $I_{zz}$, $Nms^2$: 1360;
- maximum total longitudinal thrust $T_{x1}$, N: 221;
- maximum control torque $M_{z\,\mathrm{cont}}$, Nm: 55;
- maximum stability torque $M_0$, Nm: 55.

The hydrodynamic characteristics and components of the AUV state vector were determined using a package of software applications including the following processes:

- construction of a 3D visual model of the vehicle based on the parts assembly in CAD SolidWorks;
- calculation of hydrodynamic characteristics of the model by virtual scavenging method (Flow Vision);
- solving a system of motion equations and finding the components of the state vector and controlling effects (Simulink Matlab).

The results of calculation of the hydrodynamic effects $R_x(\alpha)$, $R_y(\alpha)$, $M_z(\alpha)$ within the range of incidence angles $\pm 60°$, related to the inflow speed, are shown in Fig. 2.

The quality of control depends on the performance of actuating elements, including their specific design and limitations on the parameters of control responses. In traditional configuration, the propulsion system consists of propulsion sustainer motors ori-

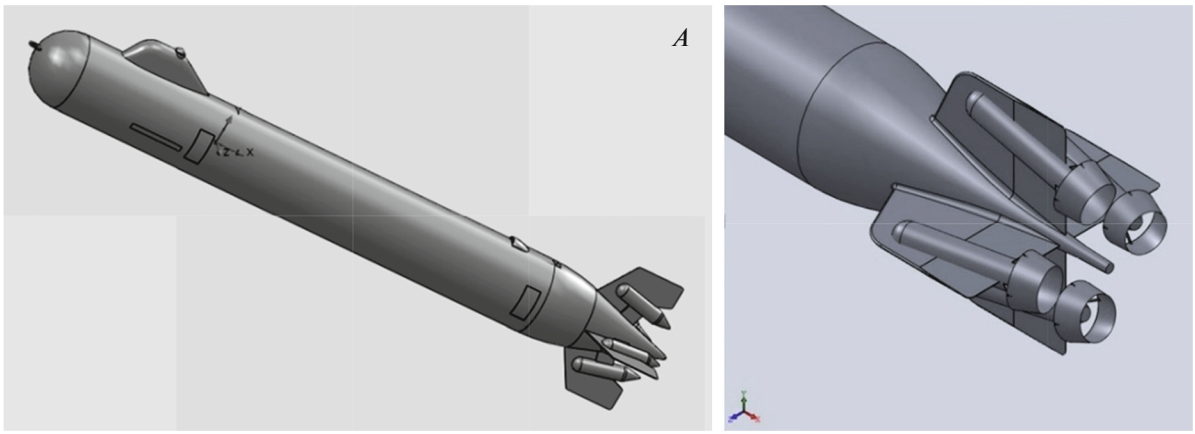


**Fig. 1.** Image of 3D model of AUV and stern propulsion system.

ented in pairs in the vehicle symmetry planes, and updraft thrusters. Such a structure makes it possible to create arbitrary thrusts and torques by varying the components of these forces. For a maneuverable multi-purpose vehicle capable of moving in various modes including positioning, hovering, start/stop steering, etc., a more efficient system is used, containing two groups of propulsion devices: four (or three) stern sustainer motors and two (or three) thrusters, distributed along the vehicle's hull. The thrusters usually serve as supporting tools in emergency or some special modes while positioning relative to a specified position. Hereinafter, we will consider forward motion with obstacle avoidance "on the move", i.e., without using the positioning mode. In this case, the efficiency of thrusters can be manifested as additional force application (creation of thrusts and torques) to overcome very steep and high obstacles. We will limit ourselves to a simpler problem and present the control responses in the vertical plane when using the stern propulsion section, as follows [1, 2]:

$$\begin{gathered} T_{x1} = (T_1 + T_2 + T_3 + T_4)\cos\gamma, \\ T_{y1} = (T_1 - T_2)\sin\gamma = T_{y1}^{\max}\,\mathrm{sat}\left(U_{\mathrm{cont}}/T_{y1}^{\max}\right), \\ M_z^{\mathrm{cont}} = T_{y1}L_{\mathrm{s}}. \end{gathered} \qquad (2)$$

In the formulas (2), $T_1$, $T_2$ are propulsion thrusts of the vertical channel; $T_3$, $T_4$ are propulsion thrusts of the horizontal channel; $T^{\max}$ is the maximum thrust; $L_{\mathrm{s}}$ is the stern section arm; $\gamma$ is the angle of stern propulsion inclination relative to the longitudinal axis of the vehicle; $U_{\mathrm{cont}}$ is the control function for the stern propulsion; sat is the linear function with limitation on the maximum magnitude.

We take two structural options of the actuating elements for comparison:

• stern propulsion complex (SPC) to control speed, depth (distance to the bottom), and heading;

• propulsion system to control speed and heading, and a pendulum device to create the control torque in vertical plane, equivalent to the controlled stability torque.

It is necessary to mention a specific feature of using a pendulum device to control the vehicle attitude. The idea of such control is based on a similarity connecting the vehicle hull stability torque $M_0 = \rho V h_0 \sin\psi$ (where $\rho$ is the water density, $V$ is the vehicle volume, and $h_0$ is metacentric height) with the torque created by a heavy pendulum. Assume that the pendulum with a weight $P_{\mathrm{P}}$ and arm $L_{\mathrm{P}}$ is suspended freely astern the vehicle so that there is no trim of the vehicle in neutral free position. The driving mechanism rotates the pendulum to some angle $\delta$ from the vehicle's normal axis which, together with the normal to the horizon, makes the trim angle $\psi$. The angle of the pendulum vertical deviation is $\overline{\delta} = \delta \pm \psi$, where the sgn "+" corresponds to counterclockwise rotation, and the sgn "–" to clockwise rotation of the pendulum (Fig. 3).

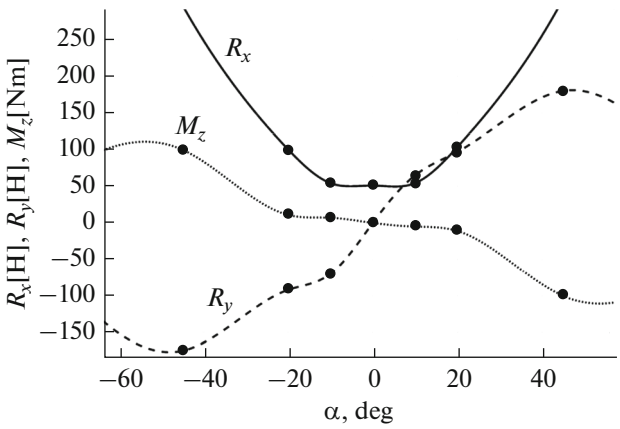


**Fig. 2.** Graphs of viscous forces versus the angle of incidence.

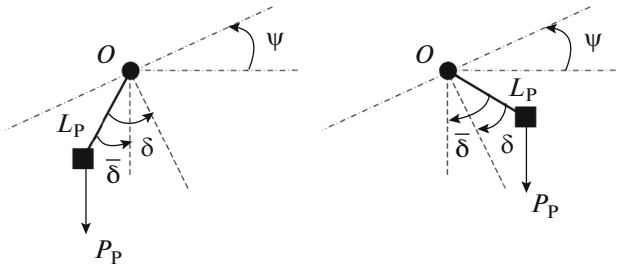


**Fig. 3.** Pendulum device diagram.

The torque $M_{z\,\mathrm{cont}} = P_P L_P \sin(\delta \pm \psi)$ created by the pendulum is equivalent to the variable stability torque, which makes it possible to interpret this effect as control by means of stability torque variation. The drive that rotates the pendulum to a specified angle can be represented by a first-order factor with input in the form of a control signal of a limited value, corresponding to the specified rate of the motor rotation (Fig. 4).

In the structural diagram shown in Fig. 4, $dY$ is position misalignment; $K_1$, $K_2$ are the gain coefficients of reference-input signal; $K_{\mathrm{mot}}$, $\tau$ are the gain coefficient and time constant of the torque motor. In particular, the following values of the system parameters were adopted: $K_1 = 10\ \mathrm{m}^{-1}$, $K_2 = 100\ \mathrm{rad}^{-1}$, $K_{\mathrm{mot}} = 0.5\ \mathrm{rad}^{-1}$, $\tau = 1.5$ s, $|\delta| \le \pi/6$, $|\bar{\delta}| \le \pi/3$, $P_P = 200$ N, $L_P = 0.2$ m.

The dynamic processes in the control system were studied using a simulation model presented in the chart in Fig. 5, where PSS is acronym for propulsion and steering system.

The main activating element in the dynamic model is the AUV model.

## AUV CONTROL SYSTEM DYNAMICS DURING NEAR-BOTTOM EQUIDISTANT MOTION

The dynamic properties of AUV control system can be estimated by analyzing the quality of transition processes while following-up the specified initial depth misalignment (Fig. 6). In further analysis of the dynamic processes, we will consider two control options: option 1 with traditional SPC control scheme, and option 2 with combined control using a pendulum device. Control in depth is based on PID controller with limited value of control responses, typical of AUV motion control systems [2–6].

Let us note some features of the system dynamics in two presented options of control with identical parameters of the PID controllers. The dynamic characteristics of the transition processes in the first option depend significantly on the value of vertical control force which is maximal at the initial time point. For this reason, significant (more than 40°) angles of incidence can be observed at relatively small vertical component of speed (0.1–0.2 m/s). Due to the large attack angles, the viscous forces and, accordingly, the control responses are fairly high, too, which naturally results in greater energy consumption for motion. In the option with a pendulum device, the angular motion is controlled by means of torques without the vertical component of force. This does not lead to large attack angles, the resistance forces are small, and the transition process attenuates quickly. This option of control has a considerable advantage in terms of the quality of transition processes while following-up the specified depth misalignments.

We assess the pattern of dynamic processes for near-bottom equidistant motion. The bottom relief profile is specified as a plane curve with "apexes" up to 25 m and slope angles up to 20°. If the bottom relief profile is known in a model under study, and if it can be specified with a function $Y(x)$, the equation of equidistant path located at a distance of $Y_{\mathrm{spec}}$ from the bot-

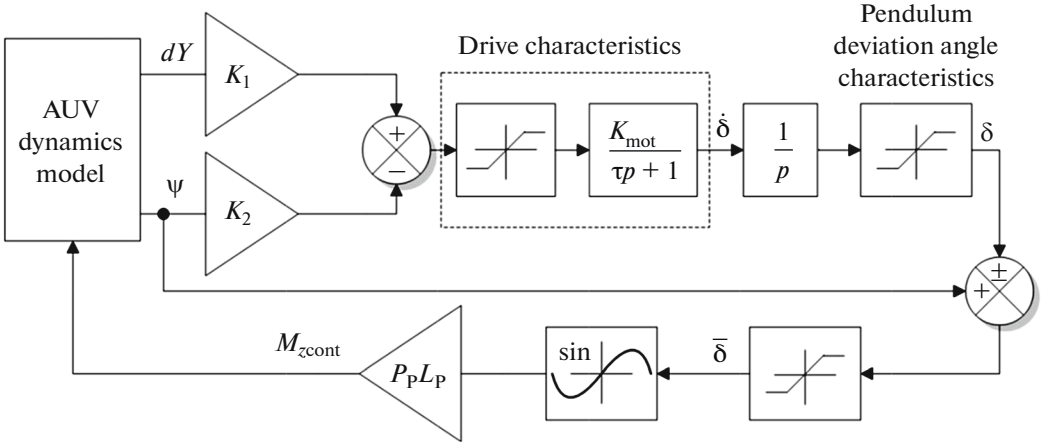


**Fig. 4.** Structural diagram of pendulum rotation control system.

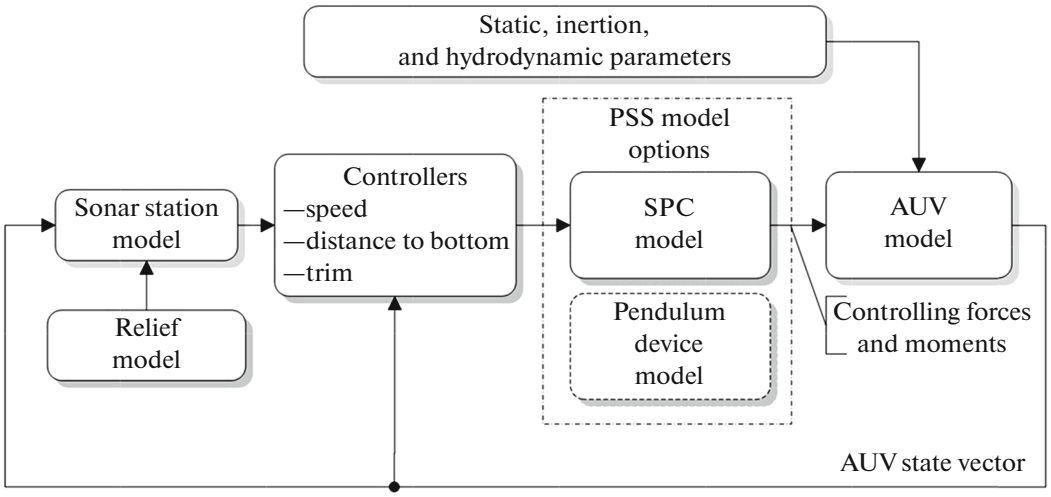


**Fig. 5.** Functional chart of AUV dynamic model.

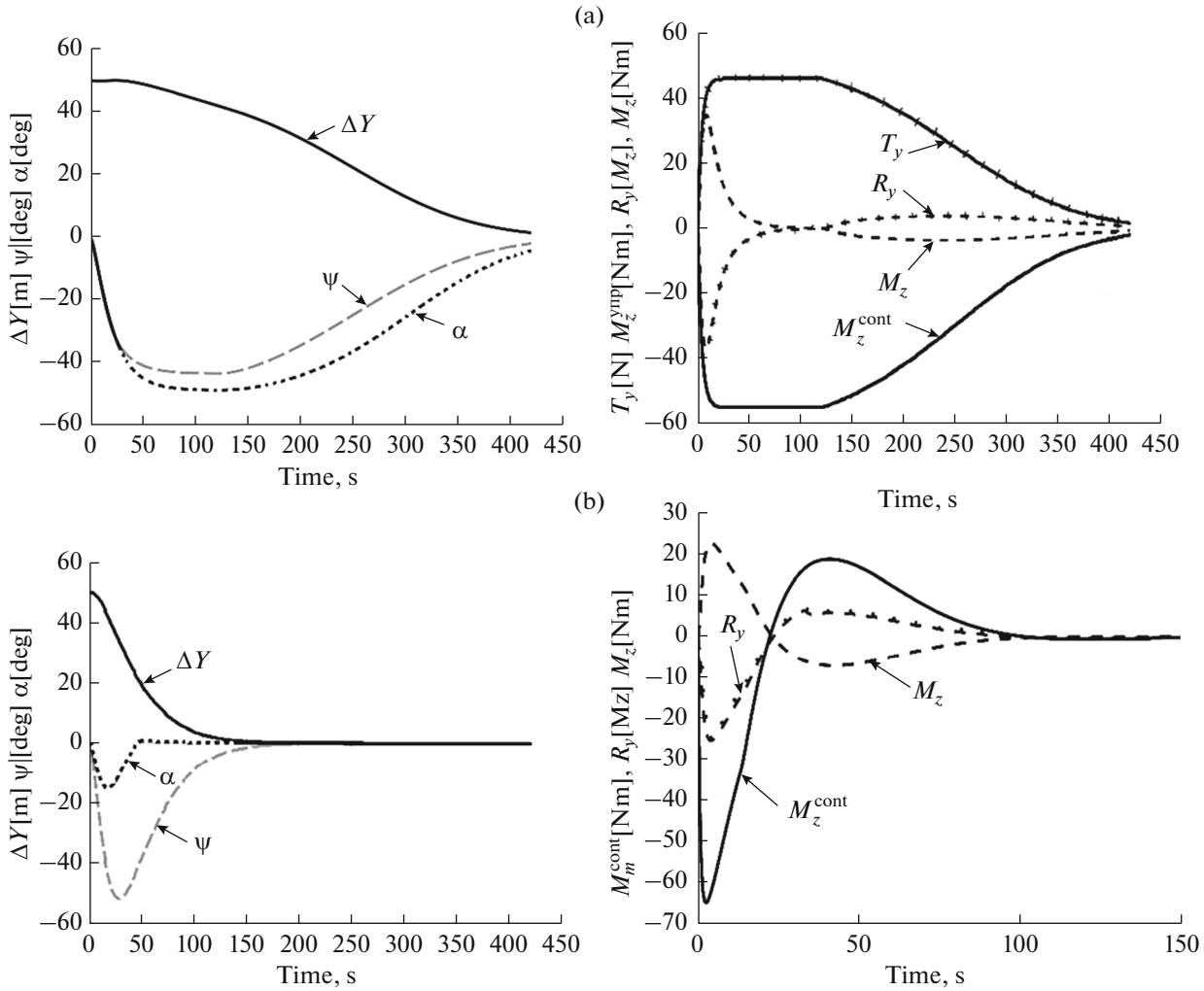


**Fig. 6.** Transition processes (left) and acting forces (right) with initial depth misalignment of 50 m with two options of actuating elements: (a) option 1, (b) option 2.

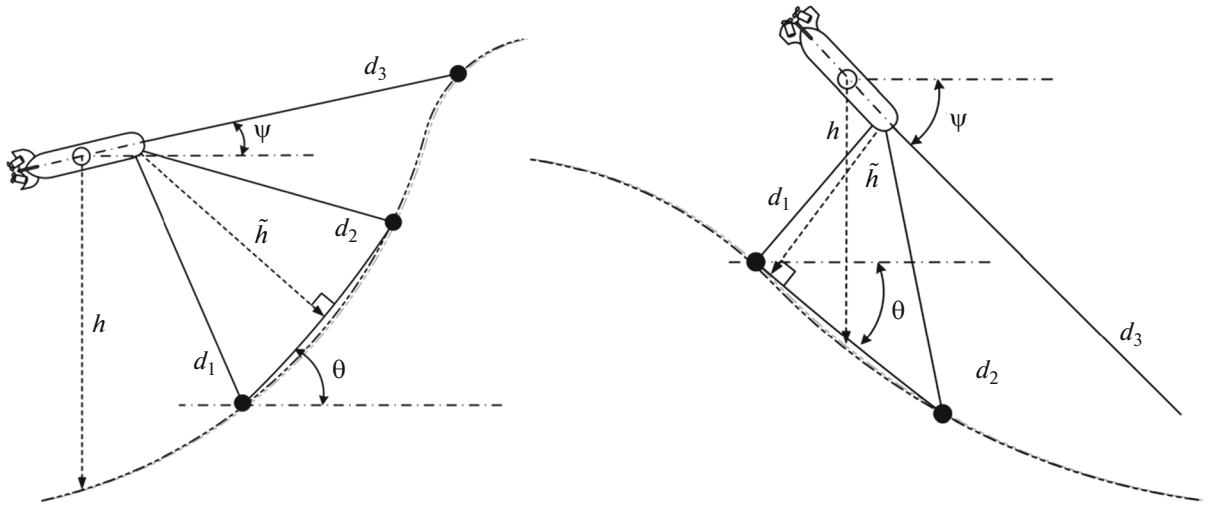


**Fig. 7.** Diagram of AUV orientation relative to the bottom relief profile.

tom surface will be in the following form: $Y(x)-Y_{\text{spec}} = 0$. In reality, the data on the bottom relief profile are formed during motion, based on sonar data, and the task is to form the control responses that ensure the motion by a trajectory close to some "predicted" equidistant path relative to the bottom. In fact, this means stabilization of vertical distance from the bottom, or the normal to the bottom surface, using the sonar station data.

It is necessary to give consideration to the features of control, relating to the equidistant path determination and measurement in course of motion. The shortest distance from the vehicle mass center to the bottom in case of variable relief can be determined by either of two values: vertical height $h$ or normal $\tilde{h}$ to the bottom surface. The difference between these two values depends on the vehicle's trim and the steepness of the slope relative to which the vehicle is moving. The task of motion stabilization along the equidistant path from the bottom is to make the vehicle trajectory repeat the relief profile with a certain accuracy, maintaining the specified distance to the bottom. This means that, when moving along a slope with variable steepness at a specified distance from the bottom, it is necessary to maintain the trajectory angle $\vartheta$ equal to the instantaneous angle of the slope. If this requirement is met, the motion proceeds with some attack angle. In case of relatively flat bottom (at small attack angles), the angular control reduces to maintaining the trim corresponding to the slope steepness.

In order to orient the AUV relative to the bottom relief and to form the equidistant-based control, a three-channel sonar station is used, where one sonar is oriented downwards (measured distance $d_1$), the second one is tilted forward at the angle φ (measured distance $d_2$), and the third one is directed forward, in the direction of motion ($d_3$). The measured distance to bottom and the normal distance are related in a trigonometric formula $\tilde{h} = d_1 \cos(\psi - \theta)$, where θ is the slope angle (Fig. 7). This value is approximately determined through the following relationship connecting the measured distances to the bottom, with trim angle and the angles between the beams of range-finders $\varphi_i$ ($i = 1, 2$):

$$\theta = \psi + (\varphi_1 + \varphi_2) - \arctan\left[(d_2 \sin\varphi_1)/(d_1 - d_2\cos\varphi_1)\right]. \quad (3)$$

In further calculations, it is assumed for specificity that $\varphi_1 = \varphi_2 = \pi/4$; therefore,

$$\theta = \psi + \pi/2 - \arctan\left[d_2/(d_1\sqrt{2} - d_2)\right].$$

For stabilizing the vehicle's steady motion by equidistant path with obstacles avoidance, a control torque is formed, which depends on positional misalignments in two sonar channels, and on the trim angle corresponding to the instantaneous angle of the slope:

$$M_z^{\text{cont}} = K_{d1}(d_1 - d_1^{\text{spec}}) + K_{d2}(d_2 - d_2^{\text{spec}}) + K_\theta(\theta - \psi), \quad (4)$$

where $d_1^{\text{spec}}, d_2^{\text{spec}}$ are the specified values of distance to the bottom in two directions, with $d_2^{\text{spec}} = d_1^{\text{spec}}\cos\varphi_1$ or, specifically, $d_2^{\text{spec}} = d_1^{\text{spec}}\sqrt{2}$ at $\varphi_1 = \pi/4$; $K_{d1}$, $K_{d2}$, $K_\theta$ are the adjustable parameters of control, the selection of which provides the required quality of dynamic processes.

The distance $d_3$ measured by the front sonar is used for controlling the motion speed when rather high and steep obstacles are detected. The speed is controlled by changing the magnitude of the longitudinal thrust:

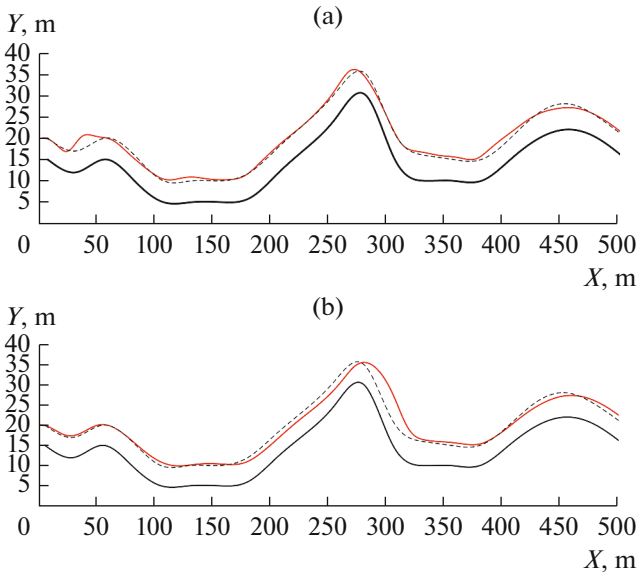


**Fig. 8.** Bottom relief profile (*black line*), specified equidistant path (*dotted line*), and two options of its implementation (*red line*): (a) option 1, (b) option 2.

$$T_{x1} = T_{x1}^{\max}\ \mathrm{sat}\left(d_3 / d_3^{\max}\right),$$

where $T_{x1}^{\max}$ corresponds to the specified speed of motion, and $d_3^{\max}$ — to the limiting value of the distance measured by the front sonar.

The results of simulation of motion along an equidistant trajectory for two options of actuating elements are shown in Figs. 9–13. The curves presented in Fig. 8 illustrate the process of bottom relief profile tracking during equidistant motion at the following values of specified parameters: $d_1^{\mathrm{spec}} = 5$ m, $d_2^{\mathrm{spec}} = 5\sqrt{2}$ m, $d_3^{\mathrm{spec}} = 50$ m, $K_{d1} = K_{d2} = 10$ m$^{-1}$, $K_\theta = 100$ rad$^{-1}$.

The pattern of equidistant motion at a small distance from the bottom is identical for both options of control; some differences can be observed only when moving around rather high and steep obstacles. These differences are caused mainly by the difference in the variation of attack angle, and by the method of slope angle identification in accordance with the formula (3). At the same time, it is important to keep in mind that the range-finders determine the "future" slope steepness on the way of motion, which appears to differ from the slope steepness under the vehicle's keel (Fig. 9). Here $\theta$ is the specified (simulated) value of the bottom relief slope angle under the vehicle's keel; $\theta_c$ is the value determined in accordance with (3). In some individual cases, these values coincide, which obviously results from the chosen control law such as (4) at the trim angles different from the calculated angle of slope. It should be noted that the value $\theta(x)$ is determined using discrete range-measuring data containing the errors of calculations in the form of specific "noise".

When tracking the specified equidistant path, the horizontal and vertical components $V_x$, $V_y$ of the motion speed change in accordance with the data on the vehicle orientation relative to the bottom relief profile (Fig. 10, a, b). It can be noted that in both options of control, the horizontal component of speed varies within 0.8–1.1 m/s depending on the obstacles on the way of motion. The vertical component of speed in both options varies more intensely in the range of –0.5–0.4 m/s depending on the bottom relief profile. During the vehicle maneuvering to avoid obstacles, interdependent variation takes place in the hydrodynamic and control responses $R_x$, $R_y$, $M_z$, $T_x$, $T_y$, $M_z^{\mathrm{cont}}$ (Figs. 11, 12). Respective variation in the angular values is shown in Fig. 13, where some differences in the system dynamics for two options of control are due to the differences in the variation of motion speed components and thus, in the variation of angular values, especially the attack angle. Energy consumption for motion depends on the type of variations in all the values described above. Simple calculations show that the power consumed for motion, with-

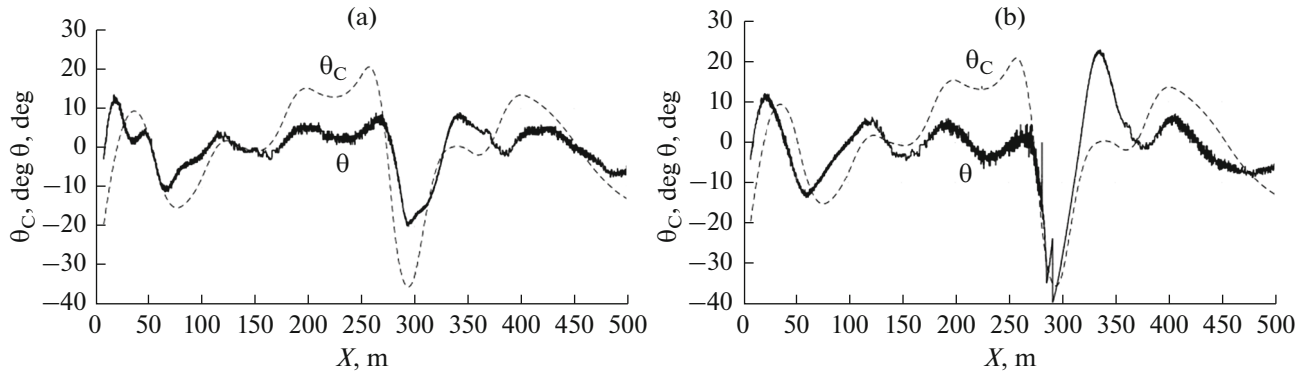


**Fig. 9.** Simulated and measured ("predicted") value of bottom relief slope angle along the motion path: (a) option 1, (b) option 2.

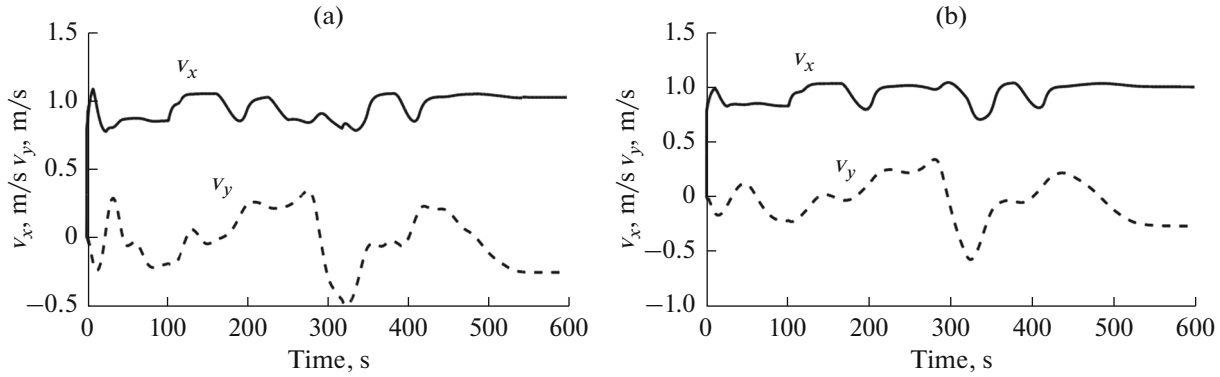


**Fig. 10.** Variations in the motion speed components $V_x$, $V_y$ at specified speed of steady motion $V = 1$ m/s: (a) option 1, (b) option 2.

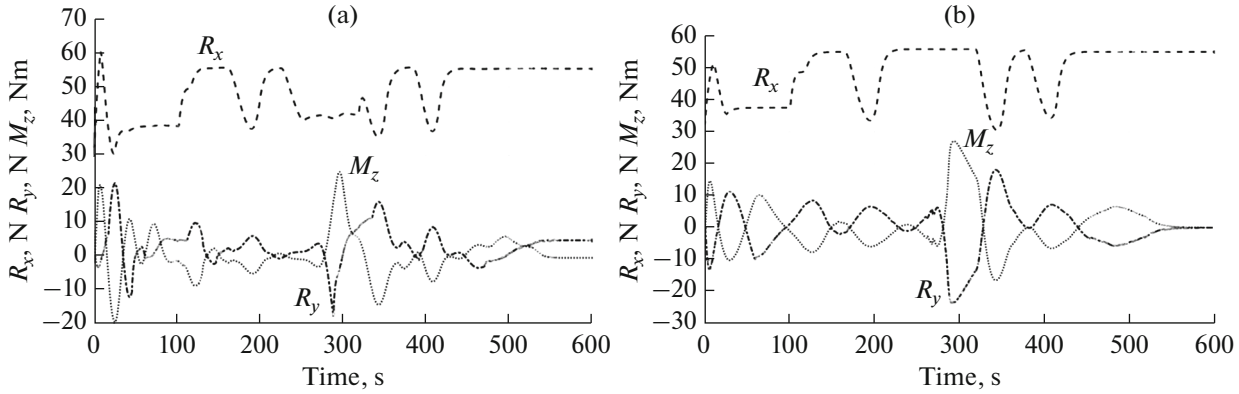


**Fig. 11.** Variations in hydrodynamic effects: (a) option 1, (b) option 2.

out taking into account the electromechanical performance of the actuating elements, amounts to 58.5 W in the first control option and 53.7 W in the second one. Evidently, during long-term operation of the AUV, the control option with pendulum device will be much more energy-saving with regard to motion.

## CONCLUSIONS

Based on the study results, the following conclusions can be drawn.

(1) The adopted models and algorithms of control of equidistant motion relative to the bottom relief, using two options of actuating elements, are efficient in the conditions of bottom relief with moderate com-

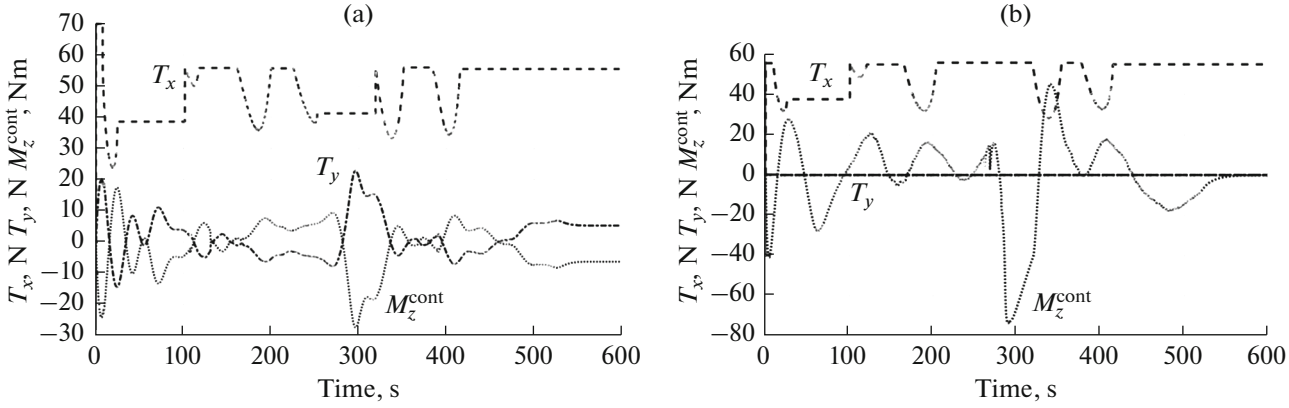


**Fig. 12.** Variations in control responses: (a) option 1, (b) option 2.

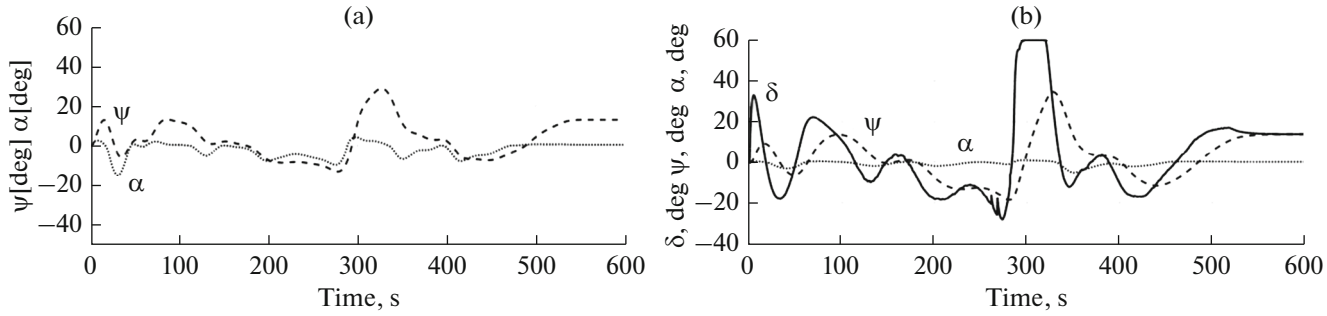


**Fig. 13.** Variations in angular values: (a) option 1, (b) option 2.

plexity, and make it possible to track the equidistant path fairly accurately "on the move", at a safe distance from possible obstacles.

(2) Obstacle avoidance is performed by setting the control responses proportional to the measured positional misalignments and angular position of the AUV relative to the bottom relief slope. At that, the control by means of the stern propulsion system while maneuvering in a variable relief is associated with rather large attack angles. The latter result in some increase in the fluid resistance forces and, consequently, in increased energy consumption during motion. In a control system with a pendulum device, the control is based on creating the pendulum torque without vertical component of the thrust, which reduces energy consumption during motion. Moreover, in this case, the control torque is equivalent to the vehicle stability torque, which provides the balance of requirements for stability and for control accuracy at any changes of the state vector.

## REFERENCES

1. Ageev, M.D., Kasatkin, B.A., Kiselev, L.V., et al., *Avtomaticheskie podvodnye apparaty* (Automatic Underwater Vehicles), Leningrad: Sudostroyeniye, 1981.
2. Ageev, M.D., Kiselev, L.V., Matvienko, Yu.V., et al., *Avtonomnye podvodnye roboty. Sistemy i tekhnologii* (Autonomous Underwater Robots. Systems and Technologies), Moscow: Nauka, 2005.
3. Inzartsev, A.V., Kiselev, L.V., Kostenko, V.V. et al., *Podvodnye robototekhnicheskie kompleksy. Sistemy, tekhnologii, primenenie* (Underwater Robotic Complexes. Systems, Technologies, Applications), Vladivostok: Dal'press, 2018.
4. Kiselev, L.V., *Kod glubiny* (Code of Depth), Vladivostok: Dal'nauka, 2012.
5. Inzartsev, A.V., Kiselev, L.V, Medvedev, A.V, and Pavin, A.M., *Autonomous underwater vehicle motion control during bottom objects and hard-to-reach areas investigation, Motion Control,* Vienna: InTech, 2010, pp. 207–228.
6. Kiselev, L.V., and Medvedev, A.V., Dynamic models for trajectory survey and mapping of local physical fields of the ocean with autonomous underwater vehicle, *Proc. of Intern. Symposium on Underwater Technology* (UT 2017), Busan, South Korea, 21–24 Feb. 2017, IEEE Xplore.
7. Pantov, E.N., Makhin, N.N., and Sheremetov, B.B. *Osnovy teorii dvizheniya podvodnykh apparatov* (Fundamental Theory of Underwater Vehicles Motion), Leningrad: Sudostroyeniye, 1973.
8. Yastrebov, V.C., Ignat'yev, M.V., Kulakov, F.M., and Mikhaylov, V.V., *Podvodnye roboty* (Underwater Robots), Leningrad: Sudostroyeniye, 1977.
9. Antonelli, G., *Underwater Robots. Motion and Force Control of Vehicle-Manipulator Systems*, *Springer Tracts in Advanced Robotics*, 2006, vol. 2.
10. Saeidinezhad, A., Dehghan, A.A., and Manshadi, M.D., Experimental investigation of hydrodynamic characteristics of a submersible vehicle model with anon-axisymmetric nose in pitch maneuver, *Ocean Engineering*, 2015, no. 100, pp. 26–34.
11. Geisbert, J.S., *Hydrodynamic Modeling for Autonomous Underwater Vehicles Using Computational and Semi-Empirical Methods*, Blacksburg, Virginia, 2007.
12. Kiselev, L.V., and Medvedev, A.V., Comparative analysis and optimization of dynamic properties of autonomous underwater robots of different projects and configurations, *Podvodnye issledovaniya i robototekhnika*, 2012, no. 1(13), pp. 24–35.
13. Kiselev, L.V., and Medvedev, A.V., On parametric relationships of hydrodynamics and motion stability of autonomous underwater robot, *Podvodnye issledovaniya i robototekhnika*, 2013, no. 1(15), pp. 33–39.